International Journal of Advances in Engineering and Management (IJAEM)
Volume 6, Issue 05 May 2024, pp: 1116-1124 www.ijaem.net ISSN: 2395-5252

# Comparative performance analysis of PI and PID controller for IPM synchronous generator under variable wind speed

Mohamed Mouloud Kadoum1, Elham Rajab Ahmed Almarjini[2]

Date of Submission: 18-05-2024 Date of Acceptance: 28-05-2024

**ABSTRACT—**This paper proposes a direct control scheme for an IPM synchronous generator-based direct drive wind turbine. The generator performance is tested with PI and PID controllers respectively. In the proposed methodology, the prerequisite of rotor position is eliminated and all the necessary calculations are performed keeping the stator frame as a reference. Direct control possesses advantages compared to the conventional control method (indirect control) such as less dependence on generator parameters, torque and flux controlled directly, and reduced number of controllers. The proposed is simulated using MATLAB/Simulink, and the results show the generator's performance with the PI and PID controllers. Then, a comparison between the two controllers is conducted.

**Keywords**: Interior permanent magnet (IPM)synchronous generator, direct control, PI controller, PID controller.

## I. INTRODUCTION

Among the different accessible renewable energy resources, wind energy is magnifying its attributes and becoming the most widely used renewable energy in power generation. It will be one of the brightest and most optimistic technologies in the future because of its eco-friendly nature, cost-effectiveness and potential to generate high power at low cost. The primary concern in wind power generation is the variation in the wind speed [1]. Two types of generators are used in large-scale wind turbines to transform wind power into electrical energy, such as a doubly fed induction generator (DFIG) and a permanent magnet synchronous generator (PMSG). PMSGs perform well in wind farms because they operate without a gearbox, and do not require excitation current [2]. They also have huge torque density, high efficacy, and reduced size and weight. IPM electric machines are also utilized for numerous applications, such as industrialized applications, domestic appliances, and electric and hybrid vehicles. They are well known because of their high efficacy, power, and torque density [3]. Moreover, another notable feature of the IPMSG-based wind generator is that the generator can be operated with an extended speed range utilizing field weakening, which will allow constant power-like operation at speeds higher than the rated speed. This work is based on an interior permanent magnet-type synchronous generator-based variable speed wind turbine [4], [5].The primary goals of the control strategies for better wind energy operation are to reduce dynamic and static mechanical loads, offer stability for grid integration, maximize power generation, and ensure a reliable grid. In this regard, power electronics (PE) play a significant role in wind systems' efficient control and optimal operation. The converter technology used in wind power applications has changed significantly over the past several years due to wind turbine systems' (WTS) rapidly increasing capacity and increasingly important effects on the electrical grid [6]. Several different topologies have been adopted over the years for PMSG-based wind generators, Different control strategies employed for permanent synchronous generator-based variable speed wind turbines such as switch-mode boost rectifiers, three-switch pulse-width modulation (PWM) rectifiers, and six-switch vector-controlled PWM rectifier. The control of PMSG-based variable speed wind turbines with switch-mode rectifiers has the merit of a simple structure and low cost because there is only one controllable switch. However, it cannot control the generator power factor and introduces high harmonic distortion, which affects the generator's efficiency. Moreover, this scheme introduces high voltage surges on the generator winding which can reduce the life span of the generator. This paper implements a direct

International Journal of Advances in Engineering and Management (IJAEM)
Volume 6, Issue 05 May 2024, pp: 1116-1124 www.ijaem.net ISSN: 2395-5252

control strategy where coordinate transformations are not required as all the calculations are done in a stator reference frame. This approach is inherently sensorless. However, a speed sensor is only required for a speed control loop [7].The PI regulators are still the widest spread controllers in the industry due to their robustness and ability and wide-range stability margins. However, PI controllers are sensitive to element changes and system nonlinearity. Therefore, optimal fine-tuning of PI controllers is the cheapest and most suitable solution in a control system of grid-connected renewable power generation [8]. A PID controller continuously calculates an error value as the difference between a measured process variable and a desired set point. The controller attempts to minimize the error over time by adjusting a control variable, such as the position of a control valve, a damper, or the power supplied to a heating element, to a new value determined by a weighted sum [9]. In this paper, the PI controller is used to test the generator's performance, and then the PID controller is used too.

## II. MODEL OF THE WIND TURBINE SYSTEM.

Power extraction in wind turbine: Wind turbines do not capture all wind energy. The output power of the wind turbine is specified by

$$Pm = \tfrac{1}{2}\rho ACp(\lambda r, \beta)x\,(Vm)^3 = \tfrac{1}{2}\rho ACp(\omega m\, R\backslash \lambda r) \quad (1)$$

where the air density is denoted by$\rho$ ($kg/m^3$), the blade swept area is notated as$A$ ($m^2$), the power coefficientis represented as $C_p$, which is a function of tip speed ratio ($\lambda_r$) and pitch angle is indicated as $\beta$ (deg.), the wind speed is signified as $V_w$ (m/s), $\omega_m$ is the rotational speed of turbine rotor in mechanical (rad/s), and the radius of the turbine is denoted by$R$(m). The tip speed ratio is expressed as

$$TSR = \lambda r = \frac{\text{Rotor tip speed}}{\text{Wind tip speed}} = w_m R_{/Vw} \quad (2)$$

The wind turbine can produce maximum power when the turbine operates at maximum $C_p$. Therefore, it is necessary to maintain the rotor speed at an optimum value of the tip speed ratio ($\lambda_{r\_opt}$). If the wind speed varies, the rotor speed should be adjusted to follow the change

$$P_{m\_opt} = \tfrac{1}{2}\rho AC_{p\_opt}\, x\, \omega_{m\_opt}/\lambda_{r\_opt} \quad (3)$$

where

$$Kopt = \tfrac{1}{2}\rho ACp\_opt\, x\, (R/\lambda r\_opt)^3 \quad (4)$$

and

$$\omega m\_opt = \omega g\_opt = (\lambda r\_opt/R)\, Vw = KwVw \quad (5)$$

The optimum torque can be given by

$$Tm\_opt(t) = Kopt\,[wm\_opt(t)]^2 \quad (6)$$

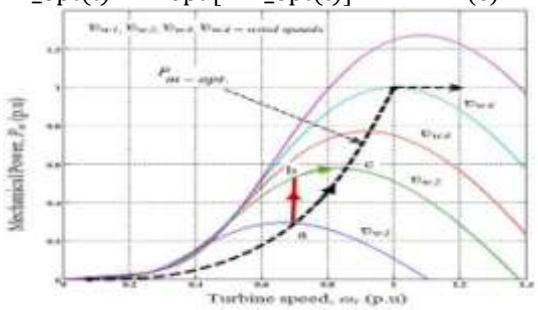


Fig 1. Graphical representation of mechanical power with respect to turbine speed under fluctuating wind speed.

In the case of wind speed variations, rotation speed always differs in such a way that optimum power is derived as shown in Figure (1). The optimized power curve provides insight into capturing the maximum energy under varying wind speeds. The turbine operates on the power curve with the help of a controller to generate maximum speed under variable wind speed conditions [10], [11].

## III. MODELING OF IPM SYNCHRONOUS GENERATOR

The Figure. 2. Shows the IPM synchronous generator direct control schema. In this schema, the torque and flux linkage is controlled directly. Two hysteresis controllers are utilized to control the torque and flux linkage and, by selecting optimum converter switching modes.The synchronous generator model is done within the stator reference frame. The machine is rotates synchronously with the rotor [12], [13].

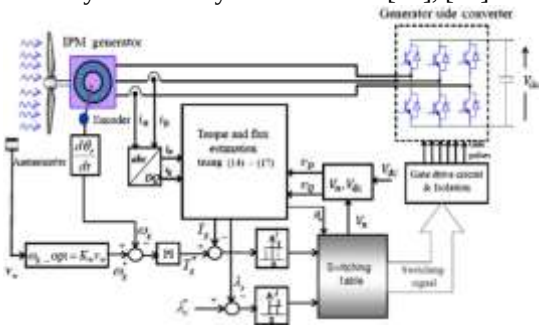


Fig. 2. Direct control schema for the IPM generator side converter.

International Journal of Advances in Engineering and Management (IJAEM)
Volume 6, Issue 05 May 2024, pp: 1116-1124 www.ijaem.net ISSN: 2395-5252

The d- axis and q- axis are used as reference signals to analyze the IPMSG model. The d- axes and q-axes voltages are tabulated as:

$$V_d = -i_d R_s - \omega_r \lambda_q + p\lambda_d \quad (7)$$

$$V_q = -i_d R_s - \omega_r \lambda_q + p\lambda_q \quad (8)$$

The flux linkages of d- axes and q-axis are tabulated as

$$\lambda_d = -L_d i_d + \lambda_m \quad (9)$$

$$\lambda_q = -L_q i_q \quad (10)$$

The equation for torque generated in IPMSG is given by

$$T_g = -\frac{3}{2}P\left(\lambda_d i_q - \lambda_q i_d\right)$$

$$= T_g = -\frac{3}{2}P\left(\lambda_m i_q - \left(L_d - L_q\right) i_d i_q\right) \quad (11)$$

where, $V_d$ , $V_q$ , $i_d$ , $i_q$ , $L_d$ , $L_q$ are the stator voltage, current and inductance for d- axis and q-axis respectively,R is the stator resistance, $\omega_r$is the rotor speed in rad/s, $\lambda_M$is the magnet flux, Pis the number of pole pairs, and ρ is the operator d/dt.

In equation (11) the first term is the excitation torque that is produced by the interaction of permanent magnet flux and$i_q$ and is independent of $i_d$. The second term is the reluctance torque that is proportional to the product of $i_d$ and $i_q$ and to the difference between $L_d$ and $L_q$. For the IPM synchronous generator, higher torque can be induced if ($L_d$ - $L_q$) is larger, while for the surface PMSG, the reluctance torque is zero since for the same $i_d$, $i_q$ if ($L_d$ = $L_q$). This is one of the advantages of an IPM synchronous generator over surface PMSG.

Figure. 3 shows the equivalent circuit for the synchronous generator with respect to d- and q-axis

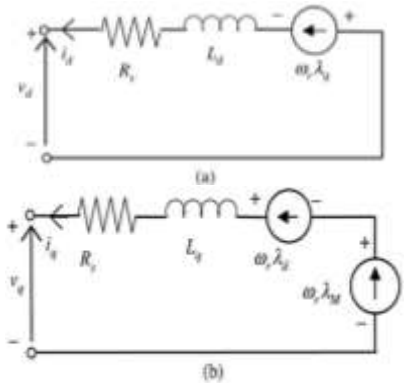

Fig 3. (a)- Equivalent circuit for (b) Equivalent circuit for d-axis q-axis.

The current references for d-q axes is given as

$$i_q = \frac{2T_g}{3P\left[\lambda_M + \left(L_d - L_q\right) i_d\right]} \quad (12)$$

$$i_q = \frac{\lambda_m}{2\left(L_d - Lq\right)} - \sqrt{\frac{\lambda_m^{\,2}}{4\left(L_d - L_q\right)} + \left(i_q^{\,2}\right)} \quad (13)$$

In the direct torque and flux control scheme, the stator flux linkage is estimated by integrating the difference between the input voltage and the voltage drop across the stator resistance expressed as

$\lambda_D = -\int (v_D - i_D R\square)dt$ (14)

$\lambda_Q = -\int (v_Q - i_Q R)\, dt$ (15)

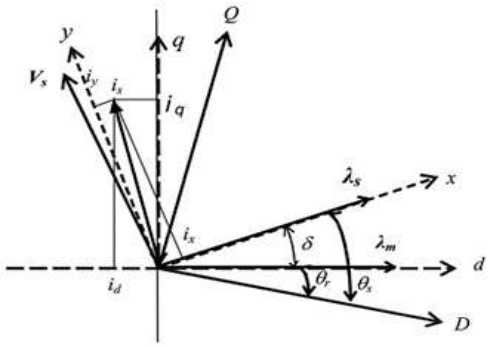


Fig 4. Stator and rotor flux linkages in different reference frames.

In the stationary reference frame, the statorflux linkage phasor is given by

$|\lambda\square| = \sqrt{\lambda_D^2 + \lambda_Q^2}$ and $<\theta = \tan^{-1}(\lambda_Q/\lambda_D)$ (16)

and the electromagnetic torque is given by

$$T_g = -\frac{3}{2}P(\lambda_D i_Q - \lambda_Q i_D). \quad (17)$$

The torque equation in terms of and generator parameters is given by

$$T_g = -\frac{3P|\lambda_s|}{4L_d L_q}(2\lambda_M L_q \sin\delta - |\lambda_s|(L_q - L_d)\sin 2\delta). \quad (18)$$

Across the IPM synchronous generator, the bidirectional power electronic switches are connected in the proposed method, as displayed in Figure 4.

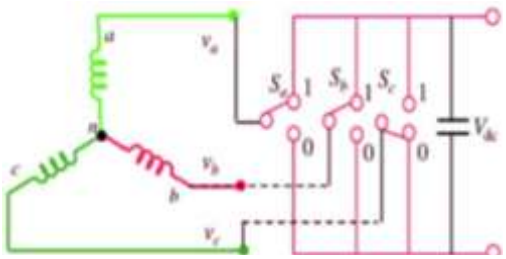

Fig 5. Rectifier connection diagram.

Six voltage vectors together with two zero voltage vectors are engendered by the rectifier. The six voltage vectors are distanced at 60 degrees apart from each other. The voltage vectors are given as

International Journal of Advances in Engineering and Management (IJAEM)
Volume 6, Issue 05 May 2024, pp: 1116-1124 www.ijaem.net ISSN: 2395-5252

$$\mathbf{v}_s(S_a, S_b, S_c) = V_D(S_a + S_b e^{j2\pi/3} + S_c e^{j4\pi/3})$$

$V_D = 2/3V_{dc}$ and $V_{dc}$ = dc-link voltage.

## IV. GENERATOR-SIDE CONTROL USING PI OR PID AND HYSTERESIS CONTROLLER.

### A. PI and PID

In the generator side converter, to maintain the generator working at an optimum situation to obtain maximum energy from wind, the speed reference ($\omega_{ref}$) is compared with the measured speed ($\omega$), and the resultant error is utilized as input to a proportional-integral (PI) or (PID) controller. The output of the PI or PID controller determines the reference torque ($T^*_{ref}$)[14], [15].

### B. Hysteresis Controller

The hysteresis control method is utilized to create the switching pulses. Because of its outstanding stability, lack of any tracking error, non-complex implementation, quick transient response, inherent restricted maximal current, and intrinsic robustness to load parameter variations. By optimizing the switching nodes, the current and generator's flux are controlled by the HCs used in the IPMSG [3]. The hysteresis control blocks compare the torque and flux references with estimated torque and flux, respectively. When the estimated torque/ flux rises above the differential hysteresis limit, the torque/flux output goes low. When the estimated torque/flux drops below its differential hysteresis limit, the torque/flux status output goes high [5].

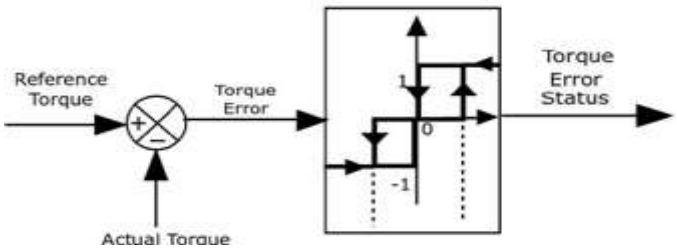


Fig 6.(a) Torque hysteresis controller.

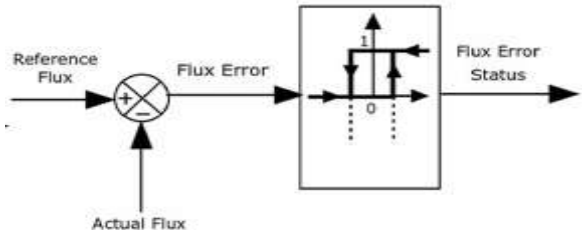


Fig 6. (b)Flux hysteresis controller.

## V. SIMULATION RESULTS AND DISCUSSION

To demonstrate the performance of the proposed control scheme, a set of simulations is carried out on an IPMSG model by using Matlab/Simulink as shown in Fig. 2. The proposed control scheme is tested under PI and PID controller.

Figure. 7 and Figure. 12 show the performance of the electromagnetic torque under PI and PID controllers respectively. In Figure. 7 the torque ripple is significant from the beginning to nearly t = 1.06 s, after that the torque ripple is reduced and arrives at a steady state at t = 1.06 s. In Figure. 12 the torque ripple is minimized and reaches stability at t = 1.1 s. Figure. 7 clearly shows that torque ripple is less with the PI controller than that of the PID controller as shown in Figure. 14.

Figure. 8 and Figure. 13 show the generator speed of the IPM synchronous generator based on the PI controller and the PID controller. Figure. 8 exhibits a better response and less speed ripple than the PID controller, which shows a higher speed ripple. Therefore, the PI controller is superior to the PID controller in regulating the speed under varying wind speeds.

Figure. 9 and Figure. 14 exhibit the three-phase voltage ($V_{abc}$) of the IPMsynchronous generator for the PI and the PID controller. In Figure. 9 from the time start of the graph to t = 1.08 s, the voltages display a high ripple, after this point, the waveform's ripple reduces and reaches a steady state specifically at t = 1.08s. In Figure 16 at time

International Journal of Advances in Engineering and Management (IJAEM)
Volume 6, Issue 05 May 2024, pp: 1116-1124 www.ijaem.net ISSN: 2395-5252

1.1s the waveform's ripple minimizes and arrives at stability. The PID controller takes a longer time to reach a steady state. That means the PI controller shows a better effectiveness than the PID controller.

Figure. 10 and Figure. 15 show the three-phase current of the IPM synchronous generator for the PI and PID controller respectively. The three-phase current in Figure. 10 displays a high ripple in the beginning and then reaches a steady state at t = 1.08s. In Figure. 15 at t = 1.1s the current arrives at stability. Then, the time stability for the PID controller is longer than the PI controller. This demonstrates the PI controller is superior to the PID controller in regulating the generator's current.

Figure. 11 and Figure. 16 show the wind turbine speed and estimated generator speed for both controllers. As shown in the Figures, the estimated generator speed closely follows the wind turbine speed quite well, even under varying wind conditions. Both controllers are able to regulate the speed for varying wind speeds but the PI controller shows a better response than the PID controller.

**A. Performance under the PI controller.**

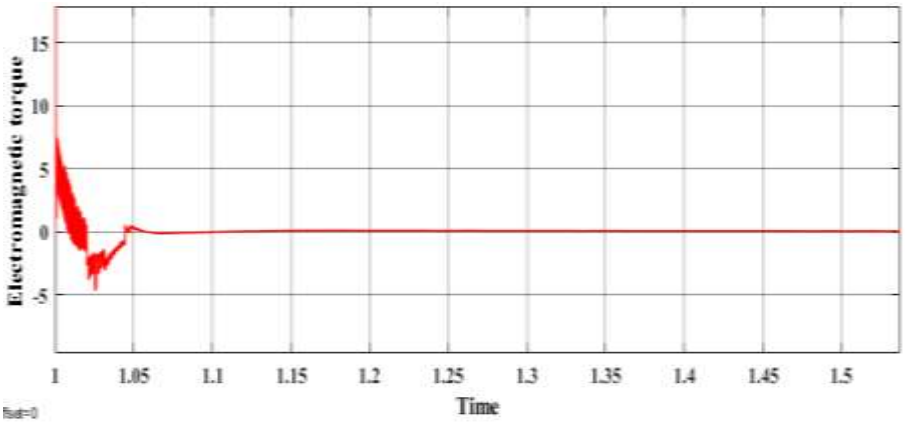


Fig 7. Electromagnetic torque of IPM synchronous generator-based PI controller.

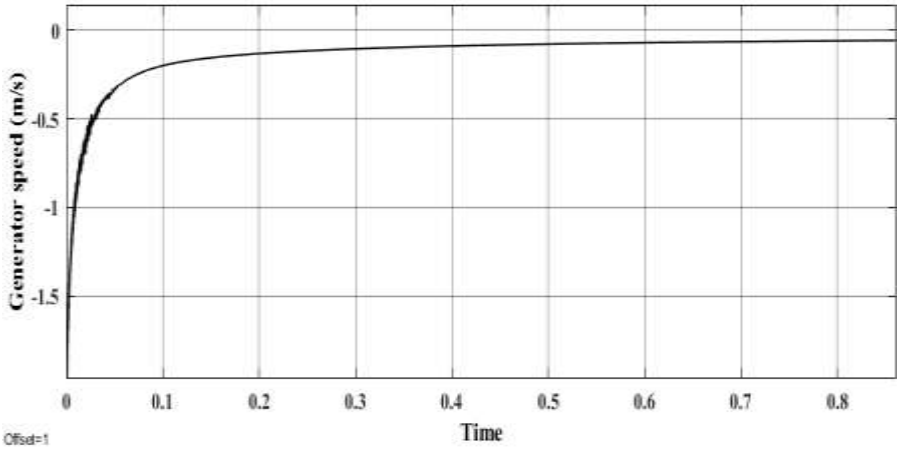


Fig 8. Generator speed of IPM synchronous generator-based PI controller.

International Journal of Advances in Engineering and Management (IJAEM)
Volume 6, Issue 05 May 2024, pp: 1116-1124 www.ijaem.net ISSN: 2395-5252

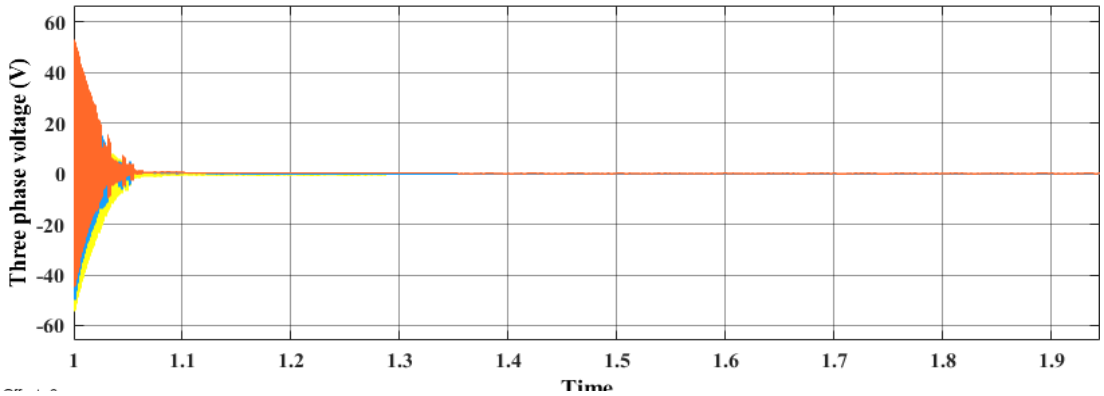


Fig. 9. Three-phase voltage of IPMsynchronous generator-based PI controller. T=1.08s

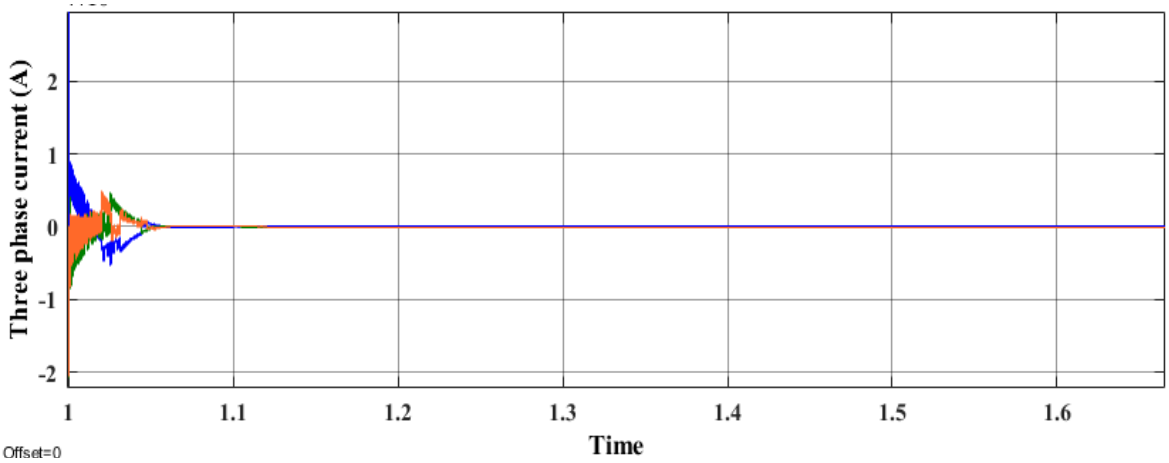


Fig 10. Three-phase current of IPM synchronous generator-based PI controller. T=1.06s

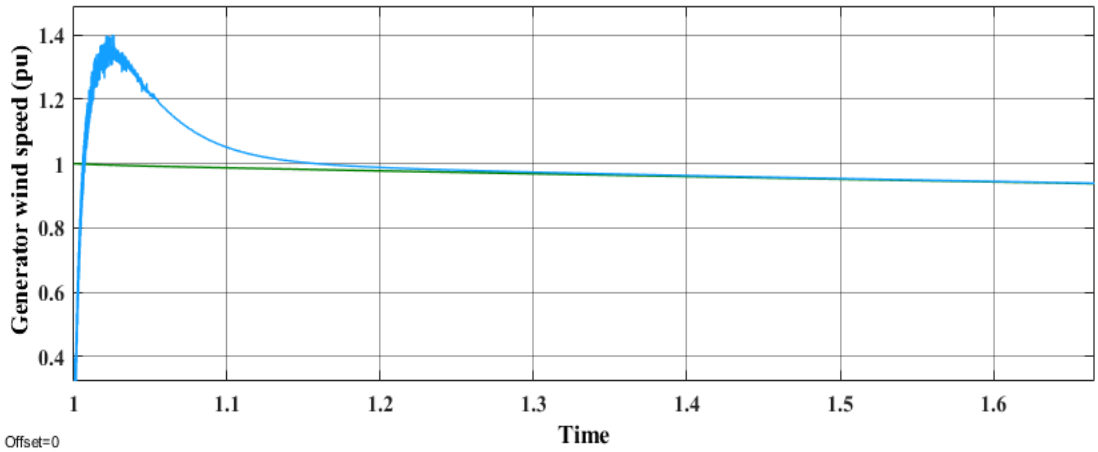


Fig 11. Estimated generator speed and estimated wind turbine speed under PI controller.

International Journal of Advances in Engineering and Management (IJAEM)
Volume 6, Issue 05 May 2024, pp: 1116-1124 www.ijaem.net ISSN: 2395-5252

**B. Performance under PID controller.**

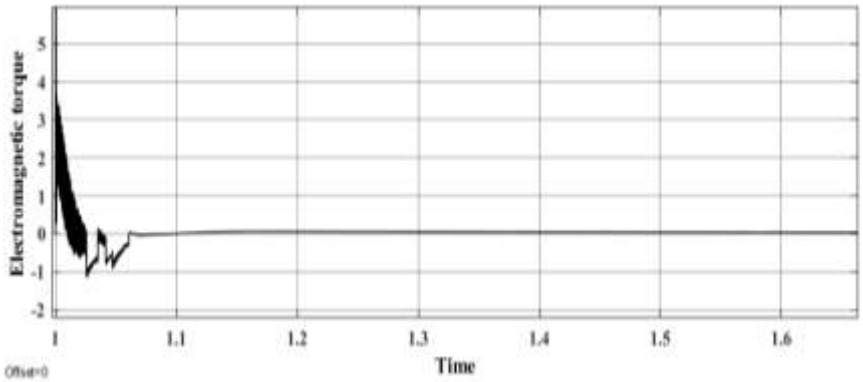


Fig 12. Electromagnetic torque of IPM synchronous generator-based PID controller.

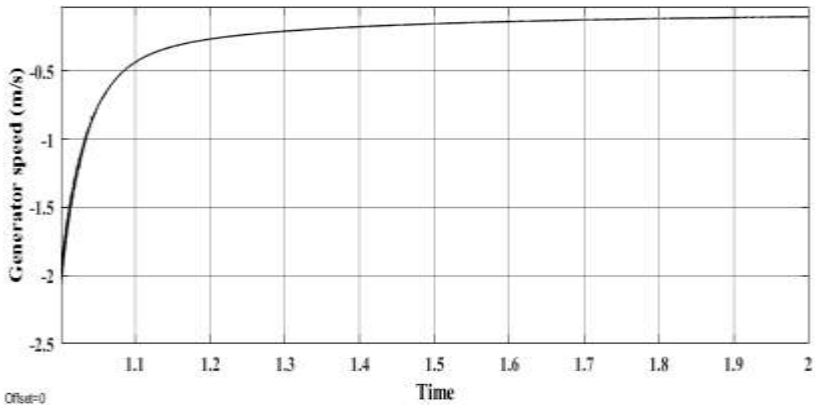


Fig 13. Generator's rotor speed of IPM synchronous generator-based PID controller.

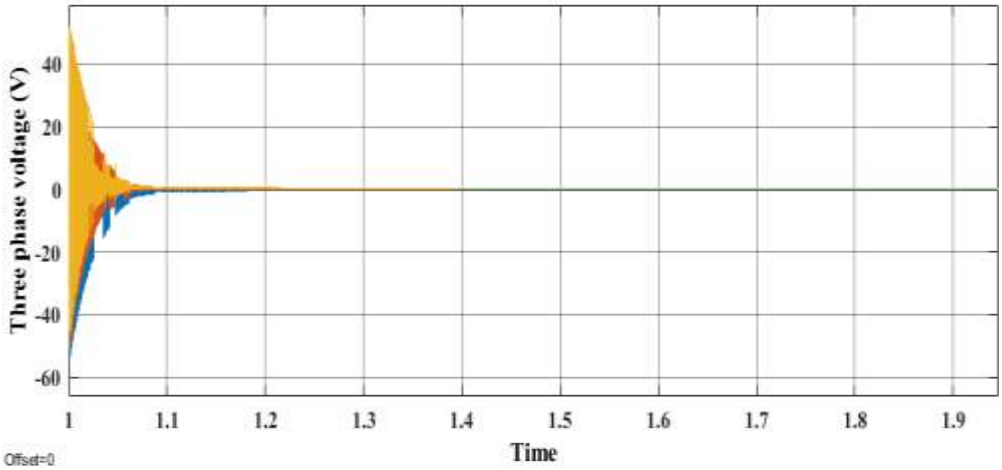


Fig. 14. Three-phase voltage of IPMsynchronous generator-based PID controller. T=1.1s

International Journal of Advances in Engineering and Management (IJAEM)
Volume 6, Issue 05 May 2024, pp: 1116-1124 www.ijaem.net ISSN: 2395-5252

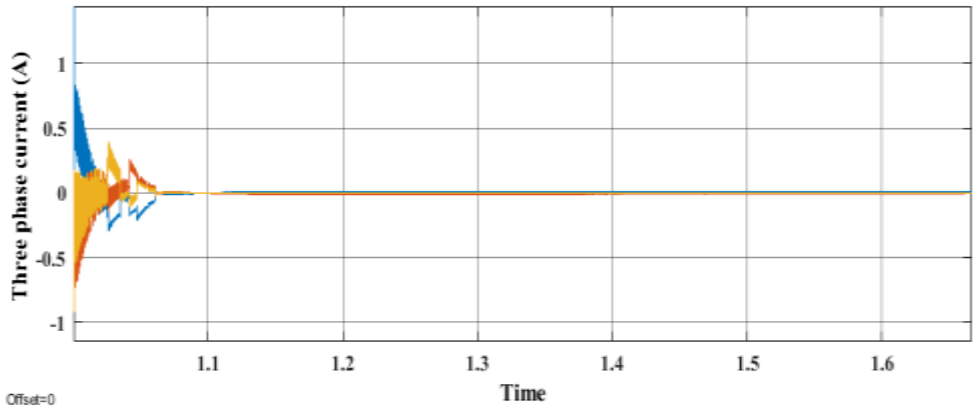


Fig 15. Three-phase current ($I_{abc}$) of IPM synchronous generator-based PID controller.t=1.1s

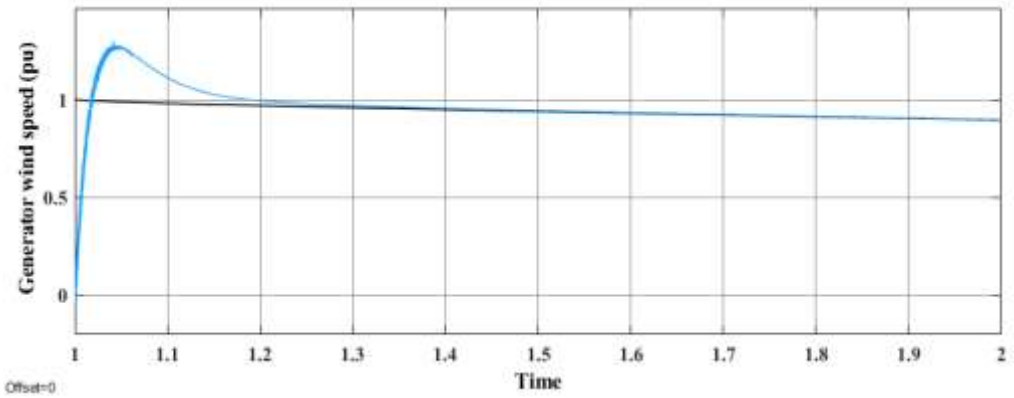


Fig 16. Estimated generator speed and estimated wind turbine speed.

## VI. CONCLUSION

This paper proposed a direct control strategy for an IPM synchronous generator based on gearless with varying wind speeds. The generator's performance was tested using the PI and the PID controllers separately. PI and PID controllers were used to obtain the torque reference. In this paper, a direct control technique was used for the IPM synchronous generator for variable speed wind energy conversion system which eliminates the prerequisite of rotor position and all the necessary calculations were done in the stator frame. The results compared PI and PID controllers under varying wind speeds. PI controller demonstrated more effectiveness than the PID controller in controlling the performance of the IPM synchronous generator.

## REFERENCES

[1]. Soliman, M. A., Hasanien, H., Azazi, H. Z., El-Kholy, E. E., & Mahmoud, S. A. (2018). An Adaptive Fuzzy Logic Control Strategy for Performance Enhancement of a Grid-Connected PMSG-Based Wind Turbine. IEEE Transactions on Industrial Informatics.

[2]. Yang, Shun, and Lida Zhang. "Modeling and control of the PMSG wind generation system with a novel controller." 2013 Third International Conference on Intelligent System Design and Engineering Applications. IEEE, 2013.

[3]. Masoud, Uossif Mohamed Matoug, Pratibha Tiwari, and Nishu Gupta. "Designing of an enhanced fuzzy logic controller of an interior permanent magnet synchronous generator under variable wind speed." Sensors 23.7 (2023): 3628.

[4]. howdhury, M. M., et al. "Control of IPM synchronous generator based direct drive wind turbine with MTPA trajectory and maximum power extraction." 2016 IEEE Power and Energy Society General Meeting (PESGM). IEEE, 2016.

[5]. Haque, M. Enamul, Y. C. Saw, and MujaddidMorshed Chowdhury. "Advanced control scheme for an IPM synchronous generator-based gearless variable speed wind turbine." IEEE Transactions on Sustainable Energy 5.2 (2013): 354-362.

[6]. Hannan, M. A., et al. "Wind energy conversions, controls, and applications: A review for sustainable technologies and directions." Sustainability 15.5 (2023): 3986.
[7]. Sharma, Shailendra, and Bhim Singh. "Control of permanent magnet synchronous generator-based stand-alone wind energy conversion system." IET Power Electronics 5.8 (2012): 1519-1526.
[8]. Qais, Mohammed H., Hany M. Hasanien, and SaadAlghuwainem. "A grey wolf optimizer for optimum parameters of multiple PI controllers of a grid-connected PMSG driven by variable speed wind turbine." IEEE Access 6 (2018): 44120-44128.
[9]. Kroičs, Kaspars, and ArvīdsBūmanis. "BLDC Motor Speed Control with Digital Adaptive PID-Fuzzy Controller and Reduced Harmonic Content." Energies 17.6 (2024): 1311.
[10]. Manna, Saibal, Deepak Kumar Singh, and Ashok Kumar Akella. "A review of control techniques for wind energy conversion system." International Journal of Engineering and Technology 13.1 (2023): 40-69.
[11]. Ghaffarzadeh, Hooman, and Ali Mehrizi-Sani. "Review of control techniques for wind energy systems." Energies 13.24 (2020): 6666.
[12]. Xu, Zhuang, and M. Faz Rahman. "Direct torque and flux regulation of an IPM synchronous motor drive using variable structure control approach." IEEE Transactions on Power Electronics 22.6 (2007): 2487-2498.
[13]. Ekanayake, Sithumini, et al. "Direct torque and flux control of interior permanent magnet synchronous machine in deep flux-weakening region." IET Electric Power Applications 12.1 (2018): 98-105.
[14]. Yang, Shun, and Lida Zhang. "Modeling and control of the PMSG wind generation system with a novel controller." 2013 Third International Conference on Intelligent System Design and Engineering Applications. IEEE, 2013.
[15]. Chowdhury, MujaddidMorshed, et al. "An enhanced control scheme for an IPM synchronous generator based wind turbine with MTPA trajectory and maximum power extraction." IEEE Transactions on Energy Conversion 33.2 (2017): 556-566.